



A ball valve micropump in glass fabricated by powder blasting

Christophe Yamahata, Frédéric Lacharme, Yves Burri, Martin A.M. Gijs*

Ecole Polytechnique Fédérale de Lausanne (EPFL), Institute of Microelectronics and Microsystems, CH-1015 Lausanne, Switzerland

Received 4 November 2004; received in revised form 4 January 2005; accepted 10 January 2005

Abstract

We present the microfabrication and characterization of a ball valve micropump in glass, which is magnetically actuated using the sinusoidal current of an external electromagnet. We employ the use of a simple powder blasting technology for microstructuring the glass substrates and fusion bonding for assembly of the multi-layered microfluidic chip. The use of a polymer membrane with embedded permanent magnet gives rise to a large actuation stroke, making the micropump bubble-tolerant and self-priming. The micropump exhibits a backpressure as high as 280 mbar and water flow rates up to 5 mL/min thanks to the large magnetic actuation force and the use of high-efficiency ball valves. The frequency-dependent characteristics are in excellent agreement with a hydrodynamic damped oscillator model.

© 2005 Elsevier B.V. All rights reserved.

Keywords: Ball valve; Micropump; Glass; Powder blasting; Magnetic actuation

1. Introduction

Pumping is one of the most common and elementary function in microfluidics. Although external (syringe or peristaltic) pumps are mostly used in laboratory experiments for the precise dispensing of fluids, the realization of miniaturized pumps has attracted attention in the development of integrated lab-on-a-chip (LOC) systems [1]. Since the first silicon micropump by van Lintel et al. [2], multiple micropumps have been reported. A majority of these are piezoelectrically actuated reciprocating pumps and are fabricated out of silicon [3–5] (the recent review of Laser and Santiago [3], in particular, gives a good overview on the topic of micropumps). Motivated by biochemical applications and the emergence of LOC systems, new devices microfabrication technologies have been developed and pumping principles, actuation methods as well as valving principles have been diversified. Unger et al. [6], for example, used soft lithography to construct multiple layer microfluidic systems containing pneumatically actuated active valves and peristaltic pumps entirely made out of silicone elastomer.

For reciprocating micropumps, magnetic actuation methods have been proposed [7,8] and plastic and glass materials have become the preferred choice [3]. In particular, glass is a very promising material for LOC applications, since it is chemically inert and sterilizable at high temperature. However, a practical self-priming glass micropump capable of delivering a high backpressure has not been reported so far. In a reciprocating micropump, a high backpressure can be achieved by a large membrane actuation force in combination with the use of high-efficiency unidirectional valves. Although ball valves are excellent candidates for the generation of unidirectional pumping flows, they have been rarely used in micropumps, probably because of their non-trivial combination with classical two-dimensional microfabrication techniques. A first type of ball valve micropump was made by stereolithography [9] and a second type was made in silicon/glass and had one active electromagnetically actuated ball valve [10]. Recently, a polymethylmethacrylate (PMMA) ball valve micropump with a pneumatically actuated membrane was reported [11].

In this paper, we have used a simple powder blasting process for the three-dimensional microstructuring of glass. The technique naturally generates conical udder-shaped holes that can be straightforwardly combined with a sphere, resulting

* Corresponding author. Tel.: +41 21 6936734; fax: +41 21 6935950.
E-mail address: martin.gijs@epfl.ch (M.A.M. Gijs).

in a high-efficiency ball valve. Glass fusion bonding was used for assembly of the multi-layered microfluidic chip. A high-temperature resistant and biocompatible polydimethylsiloxane (PDMS) membrane with embedded permanent magnet was plasma-bonded with the glass structure giving rise to a large actuation stroke, making the micropump bubble-tolerant and self-priming. We obtained a backpressure as high as 280 mbar and water flow rates up to 5 mL/min thanks to the large magnetic actuation force and the use of the ball valves. The frequency-dependent flow characteristics are explained using a hydrodynamic damped oscillator model.

2. Working principle and design

Our micropump is of the reciprocating type (see Fig. 1a): the oscillation of a flexible diaphragm results in the periodic increase and decrease of the pumping chamber volume. Two passive ball valves are placed at the entrance and exit of the pumping chamber to rectify the pulsed flow. The actuation of the PDMS membrane with embedded permanent magnet was done using an external electromagnet fed by a sinusoidal current. The microfluidic circuit which is necessary to operate the micropump with the two ball valves was based on the three-dimensional micromachining and subsequent bonding of three glass layers (see Fig. 1b).

3. Microfluidic chip fabrication

3.1. Powder blasting erosion process

Powder blasting has been demonstrated to be a low cost tool for the microfabrication of micromechanical [12] and microfluidic [13] devices in brittle materials. For all our experiments, we used an ‘HP-2 Texas Airsonics’ abrasive jet machine connected to a pressurized air source. The eroding powder consists of 30 μm size alumina particles (Al_2O_3) and was dosed to a 2 mm wide exit nozzle by a vibration feeder in an air jet. We have always applied a pressure of 3 bar to the nozzle; the distance from the nozzle exit to the substrate was 8 cm. In our experiments, we have used *Borofloat*[®] 33 borosilicate glass (Schott AG, Mainz, Germany).

When the glass wafer is covered by an erosion-resistant polymer mask, containing a circular aperture, the hole eroded in the glass has a rounded shape originating from the reduced normal impact of the particles near the mask edge [14,15]. Fig. 2a and b shows the time evolution of a hole made with a 1 mm wide mask aperture, obtained using a static powder beam. After about 20 s, a udder-like erosion profile develops at the bottom of the hole, resulting from the secondary impact of particles that are reflected from the side wall of the hole (see arrows in Fig. 2a). Evidently, this ‘natural’ shape is ideal for the realization of a ball valve seat.

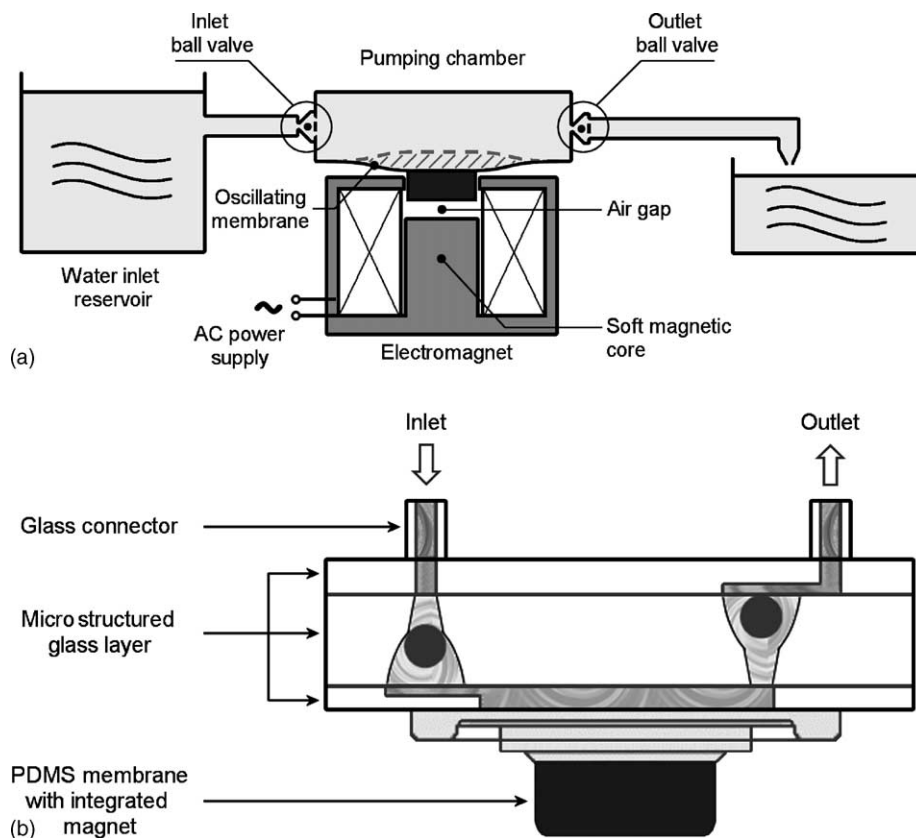


Fig. 1. (a) Schematic diagram of the ball valve micropump with external electromagnetic actuation of the magnetic membrane. (b) Principle of the glass trilayer ball valve micropump.

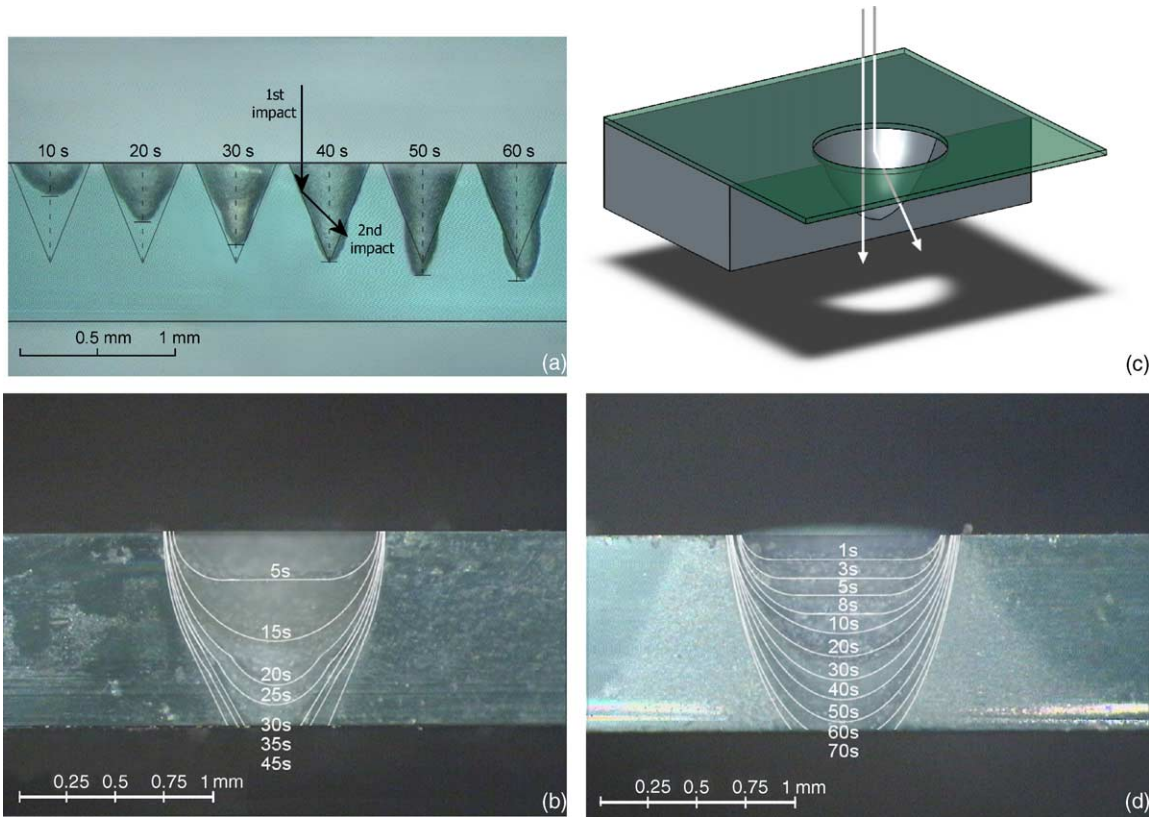


Fig. 2. (a) Evolution of the erosion profile in glass material; (b) obtained profiles in the presence of the secondary impact effect and (d) without rebounding effect. Experimental data of (d) were obtained by positioning the mask aperture at the edge of the substrate, as illustrated in (c).

The essential role of the secondary particle impact can be illustrated by positioning the mask aperture at the edge of the substrate, as shown in Fig. 2c. In this case, the particle's secondary impact is eliminated, as proven by the time-dependent erosion profiles of Fig. 2d. In Fig. 3, we report the time-dependent hole depth obtained from the experimental results represented in Fig. 2b and d. The full curve confirms the theoretical model form Slikkerveer and in't Veld [14], which only takes into account the primary impact of particles.

3.2. Glass fusion bonding

Our glass bonding process was based on the bonding experiments of Solignac [16]. After cleaning the glass plates with isopropanol and a Piranha solution, the different layers were stacked and aligned together. Finally, we carried out a high-temperature fusion bonding step of the assembly at 600 °C [17]. The thermal treatment process is given in Fig. 4.

Three glass layers have been successfully bonded in a single step by this method. One should note that this bonding is only possible with materials having very close thermal ex-

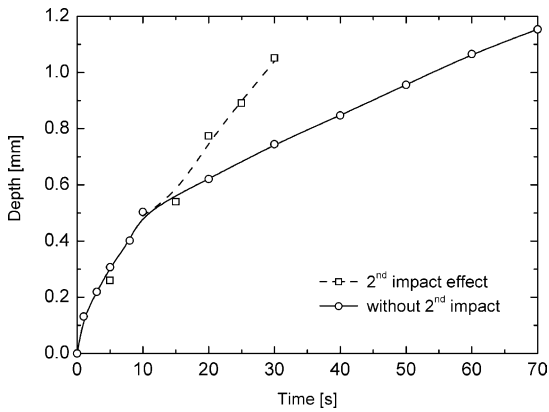


Fig. 3. The depth of powder blasted holes as a function of time in the case of second impact effect (dotted line) and without the second impact of particles (full line).

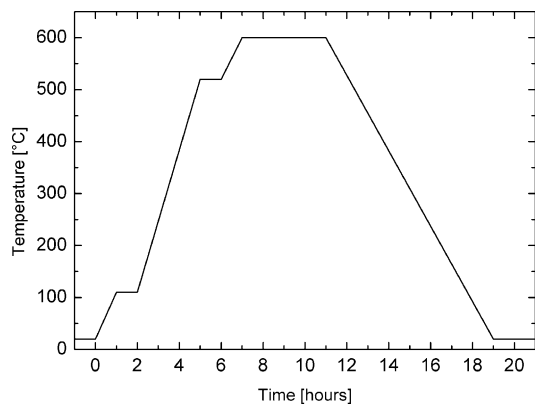


Fig. 4. Thermal treatment for borosilicate glass substrates.

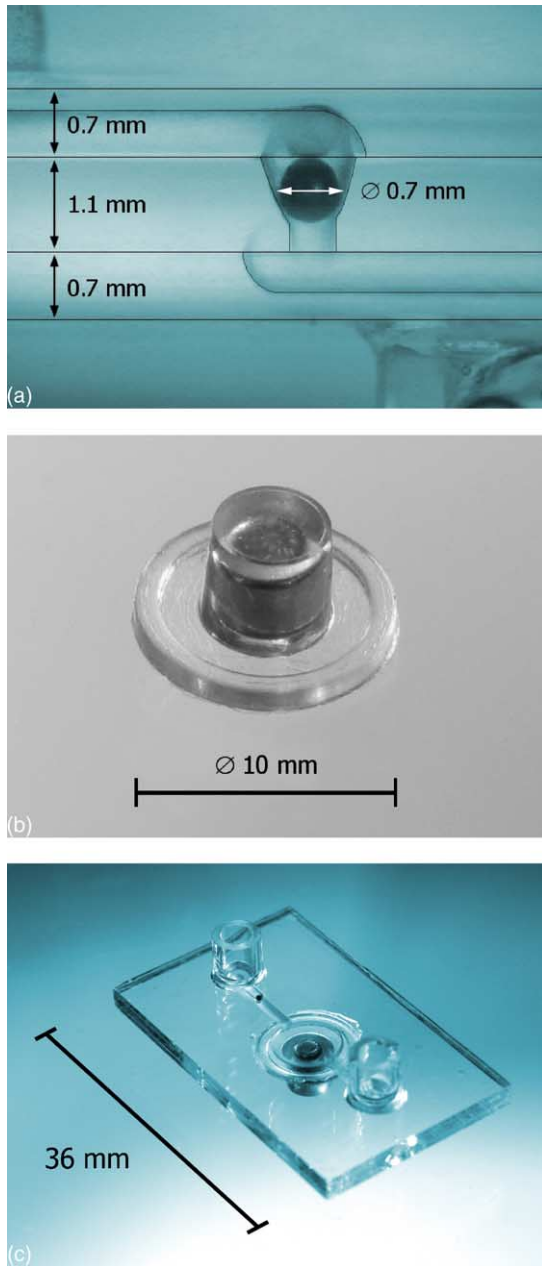


Fig. 5. (a) Photograph of the integrated ball valve. We distinguish the three different layers which are 0.7 mm (bottom and top) and 1.1 mm (middle) thick. (b) PDMS membrane with embedded rare earth magnet. (c) Photograph of the ball valve micropump.

pansion coefficients. Fig. 5a shows a photograph of an assembled ball valve made by micropatterning and fusion bonding of three glass substrates. The sphere was a $\text{Ø}0.7$ mm stainless steel ball (Kellenberg Roll-Technik AG, Oetwil am See, Switzerland).

3.3. Membrane fabrication and final assembly

In order to have reliable pumping, self-priming and bubble tolerance of the pump, a flexible membrane with large deflection amplitude is important [18]. The PDMS elastomer

Sylgard 184 (Dow Corning Corp., Midland, Michigan, USA) has been chosen for its high flexibility and its compatibility with a hot sterilization treatment (130°C). For actuation of the membrane, we have chosen a cylindrical *NdFeB/N48* (Maurer Magnetic AG, Grüningen, Switzerland) neodymium rare-earth permanent magnet ($\text{Ø}3$ mm, height = 3 mm, remanence $B_r = 1.42$ T), the magnetic properties of which are not affected by the heat treatment. We integrated the magnet in the membrane using a two-step molding process. We first partially filled a first mold with the PDMS solution and centered the magnet with a counter-piece. After partial polymerization of the PDMS, the magnet remained entrapped and the molding process could be completed using a second mold. The final membrane (see Fig. 5b) had an external diameter of 10 mm, a dimension which was higher than the diameter of the chamber ($\text{Ø}_m 7$ mm) for bonding to the glass stack. The membrane rigidity was measured to be $K = 800$ N/m, corresponding to a diaphragm spring constant $K_p = K/A_m = 20$ MPa/m, where A_m is the membrane surface. The membrane weight is $M_m = 0.25$ g.

The PDMS membrane was plasma-bonded on the glass surface using a ‘*Scancoat Six*’ plasma treatment machine (BOC Edwards, Crawley, UK). The surface of the glass substrate was first treated with an air plasma for 60 s at 0.4 mbar and 20 mA (500 V). The PDMS membrane was subjected to the same plasma treatment, but only for 10 s. After a thermal annealing at 100°C , a hermetic and irreversible bonding between the glass and the PDMS was then obtained.

For the fluidic connections to the chip surface, cylindrical glass connectors were polished and glued with epoxy solution at 80°C for 2 h (*Epo-Tek 301-2*, Epoxy Technology Inc., Billerica, Massachusetts, USA). Fig. 5c shows a photograph of the assembled glass ball valve micropump. The external dimensions of the chip are $36\text{ mm} \times 22\text{ mm} \times 2.5\text{ mm}$.

4. Results and discussion

4.1. Ball valve characterization

The flow rectification efficiency of the ball valve was evaluated on a separate device and its static flow rate–pressure characteristic is shown in Fig. 6. The fluidic resistance in the forward direction is measured to be $R_d = 3 \times 10^{10}$ N m $^{-5}$ s. Knowing that the overall dimension of the fluidic access channel to the ball valve is $22\text{ mm} \times 1\text{ mm} \times 0.4\text{ mm}$ and assuming a laminar Hagen–Poiseuille flow, the total theoretical fluidic resistance is then $R_c = 8.4 \times 10^9$ N m $^{-5}$ s (rectangular duct). If we do not take into account the resistive effect of the channels, we can evaluate from Fig. 6 the valve efficiency ε as the ratio of the flow rates in the forward and reverse direction for a given differential pressure:

$$\varepsilon = \frac{Q_+(P)}{Q_-(-P)} \approx \frac{20\text{ mL/min}}{0.25\text{ mL/min}} = 80 \quad (1)$$

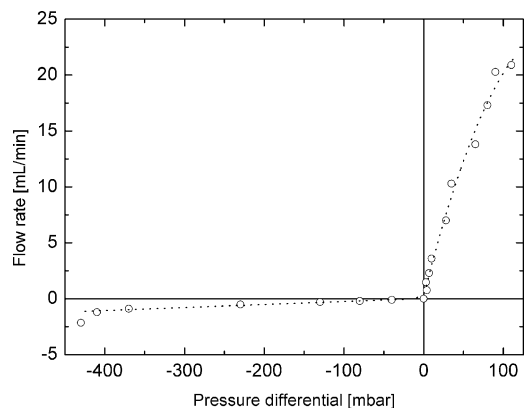


Fig. 6. Water flow rate–pressure characteristic of the ball valve.

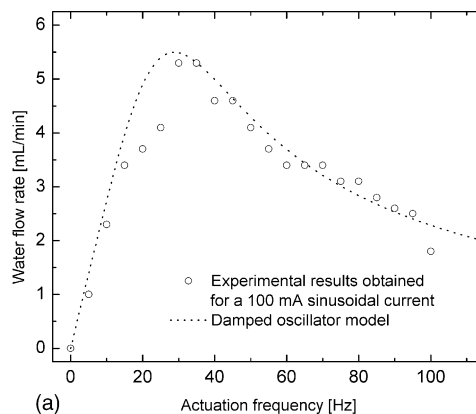
where Q_+ and Q_- are the flow rates in the forward and reverse direction, respectively and P the differential pressure applied to the ball valve.

4.2. Micropump characterization

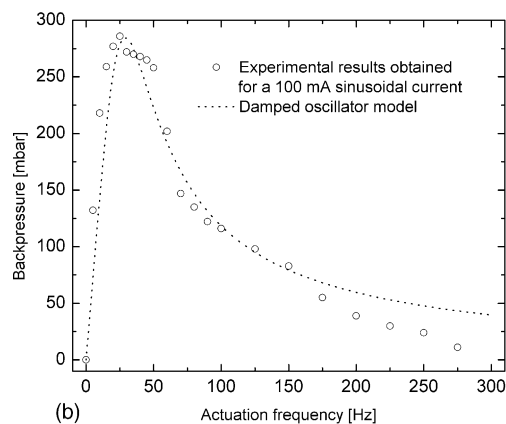
For the actuation of the micropump, a 100 mA sinusoidal current was applied to a 4800 turn commercial coil having an internal resistance of 370 Ω (Atam Windings s.r.l., Agrate Brianza, Italy). To focus and amplify the magnetic field, a soft magnetic iron core was placed into the centre of the coil. Fig. 7a represents the water flow rate characteristic of the pump measured for different actuation frequencies of the electromagnet. A flow rate of about 5 mL/min was measured at $f=30$ Hz, which is the resonance frequency of the pump. In Fig. 7b, we report the maximum obtained backpressure (at no flow rate) versus frequency for a 100 mA sinusoidal excitation of the electromagnet. At resonance, a maximum pressure of 280 mbar was measured using a pressure sensor connected to the outlet of the chip. The water flow rate–backpressure characteristic of the ball valve micropump is shown in Fig. 7c for an actuation frequency $f=30$ Hz. The hydrostatic backpressure was generated with a column of water. The linear-like decrease of the flow rate with backpressure can be explained by the fact that the flow is proportional to the difference between the mean pressure developed by the membrane in the pumping chamber and the external pressure.

4.3. Damped oscillator model of the ball valve micropump

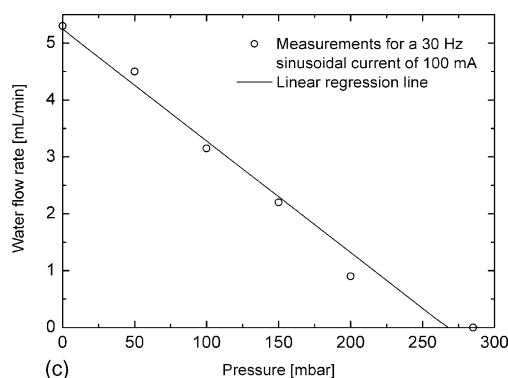
The ball valve reciprocating pump can be described with a second order damped oscillator model. This description was also used for modelling reciprocating micropumps by lumped electrical equivalent circuits [19,20]. The liquid in the channels induces both a resistive and an inertial effect. The membrane plays the role of a capacitance and its inertial effect is limited in comparison with the fluid inertia. For simplification of the model, we are assuming that the valves are ideal diodes.



(a)



(b)



(c)

Fig. 7. (a) Water flow rate–frequency characteristic of the micropump. The dotted line is obtained using Eq. (2) and the parameters of Table 1. (b) Backpressure–frequency characteristic of the micropump. The dotted line is calculated using the frequency dependence of Eq. (2). (c) Water flow rate–backpressure characteristic of the micropump actuated at 30 Hz. The full line is a linear regression curve. For all measurements, a sinusoidal actuation current with an amplitude of 100 mA was used.

Table 1 summarizes the equivalence of the hydraulic system with a simple electrical RLC model [19]. We can now calculate the values of the different parameters for our micropump, as listed in Table 1, using the following parameters: V is the pumped volume, $\rho=1000$ kg m^{-3} the density of water, $\eta=1.0 \times 10^{-3}$ N m^{-2} s the dynamic viscosity of water, $l=6$ mm the outlet microfluidic channel length, $w=1$ mm the microfluidic channel width, $h=0.4$ mm the microfluidic channel depth, A the channel cross section and D_H the

Table 1
Equivalence of the hydraulic system with the electrical model

Fluidic model	Calculated parameter/comment
Pressure, P	Equivalent to voltage
Flow rate, $\phi = \frac{dV}{dt}$	Equivalent to current
Fluid resistor, $R = \frac{128\eta l}{\pi D_H^4}$	$4.4 \times 10^9 \text{ N m}^{-5} \text{ s}$
Fluid capacitor, $C = \frac{dV}{dP} = \frac{A_m^2}{K}$	$1.85 \times 10^{-12} \text{ m}^5 \text{ N}^{-1}$
Fluid inductor, $L = \frac{\rho l}{A}$	$1.5 \times 10^7 \text{ kg m}^{-4}$
Valve	Diode (see characteristic of Fig. 6)

hydraulic channel diameter (estimated from w and h for a rectangular duct with rounded corners).

The dependence of the normalized flow rate of the pump Q/Q_0 on membrane pulsation ω is given in the following equation [20]:

$$\frac{Q(\omega)}{Q_0} = \sqrt{\frac{\omega^2}{\omega^2 + \left(\frac{L}{R}\omega^2 - \frac{1}{RC}\right)^2}} \quad (2)$$

The dotted curve in Fig. 7a is directly calculated from Eq. (2), using the parameters of Table 1. The calculated resonance frequency is $f_0 = 30$ Hz. Although only the damping effect of the fluidic channel was taken into account, the calculated position and width of the resonant peak are in agreement with the experimental data. The frequency dependence of the outlet pressure data of Fig. 7b can be described by an expression with similar frequency dependence as Eq. (2). We can finally note from these data that the micropump shows optimum behaviour at the resonance frequency of the fluidic circuit [20].

5. Conclusion

We have presented an original, simple and low-cost fabrication method for the development of a glass microfluidic ball valve pump. The use of a polymer membrane with embedded permanent magnet gives rise to a large actuation stroke, making the micropump bubble-tolerant and self-priming. The micropump exhibits a backpressure as high as 280 mbar and the water flow rates up to 5 mL/min. The frequency-dependent characteristics are in good agreement with a hydrodynamic damped oscillator model. We can anticipate that the excellent characteristics of our micropump, thanks to the use of high-efficiency ball valves and a high-deflection magnetic membrane, will lead to an advantageous use of such a type of pump in lab-on-a-chip applications, especially when chemical inertness and sterilizability are issues.

Acknowledgement

We are grateful to the Swiss Commission for Technology and Innovation which provided the funding of this work (Project CTI-MedTech 4960.1 MTS).

References

- [1] F.E.H. Tay, W.O. Choong, in: F.E.H. Tay (Ed.), *Microfluidics and BioMEMS Applications*, Kluwer Academic Publishers, Boston, 2002, pp. 3–140.
- [2] H.T.G. van Lintel, F.C.M. van De Pol, S. Bouwstra, *Sens. Actuators A* 15 (2) (1988) 153–167.
- [3] D.J. Laser, J.G. Santiago, *J. Micromech. Microeng.* 14 (6) (2004) R35–R64.
- [4] P. Woias, *Micropumps—past, progress and future prospects*, *Sens. Actuators B*, doi: 10.1016/j.snb.2004.02.033.
- [5] N.T. Nguyen, X.Y. Huang, T.K. Chuan, *ASME J. Fluid Eng.* 124 (2) (2002) 384–392.
- [6] M.A. Unger, H.-P. Chou, T. Thorsen, A. Scherer, S.R. Quake, *Science* 288 (5463) (2000) 113–116.
- [7] C. Yamahata, C. Lotto, E. Al-Assaf, M.A.M. Gijs, *A PMMA valveless micropump using electromagnetic actuation*, *Microfluidics and Nanofluidics*, doi: 10.1007/s10404-004-0007-6.
- [8] C. Yamahata, M.A.M. Gijs, *Proceedings of the 17th IEEE MEMS Conference*, Maastricht, The Netherlands, 2004, pp. 458–461.
- [9] M.C. Carrozza, N. Croce, B. Magnani, P. Dario, *J. Micromech. Microeng.* 5 (2) (1995) 177–179.
- [10] O. Krusemark, A. Feustel, J. Müller, *Proceedings of the Micro-TAS'98*, Banff, Canada, 1998, pp. 399–402.
- [11] A. Sin, C.F. Reardon, M.L. Shuler, *Biotechnol. Bioeng.* 85 (3) (2004) 359–363.
- [12] E. Belloy, S. Thurre, E. Walckiers, A. Sayah, M.A.M. Gijs, *Sens. Actuators A* 84 (3) (2000) 330–337.
- [13] D. Solignac, A. Sayah, S. Constantin, R. Freitag, M.A.M. Gijs, *Sens. Actuators A* 92 (1–3) (2001) 388–393.
- [14] P.J. Slikkerveer, F.H. in't Veld, *Wear* 233–235 (1999) 377–386.
- [15] P.J. Slikkerveer, P.C.P. Bouten, F.C.M. de Haas, *Sens. Actuators A* 85 (1–3) (2000) 296–303.
- [16] D. Solignac, *Glass Microchips for Bio-chemical Analysis: Technologies and Applications*, Ph.D. Thesis of the Swiss Federal Institute of Technology Lausanne (EPFL), Switzerland, 2003.
- [17] C. Yamahata, F. Lacharme, M.A.M. Gijs, *Glass valveless micropump using electromagnetic actuation*, *Microelectr. Eng.*, doi: 10.1016/j.mee.2004.12.018.
- [18] M. Richter, R. Linnemann, P. Woias, *Sens. Actuators A* 68 (1–3) (1998) 480–486.
- [19] T. Bourouina, J.-P. Grandchamp, *J. Micromech. Microeng.* 6 (4) (1996) 398–404.
- [20] O. Francais, S. Bendib, *SPIE Conference Proceedings on Design, Characterisation, and Packaging for MEMS and Microelectronics II*, vol. 4593, 2001, pp. 292–298.

Biographies

Christophe Yamahata was born in Paris, France, in 1977. He obtained his degree in Microengineering from the Swiss Federal Institute of Technology Lausanne (Ecole Polytechnique Fédérale de Lausanne) in 2000. He joined the Institute of Microelectronics and Microsystems in 2001 as a research assistant where he completed a Ph.D. thesis on the subject of

“Magnetically Actuated Micropumps” in 2005. He is currently pursuing research at the University of Tokyo, as a postdoctoral fellow of the Swiss National Science Foundation.

Frédéric Lacharme was born in Bordeaux, France, in 1978. In 2002, he obtained a Master degree in physical chemistry from the University of Bordeaux 1. He is currently a Ph.D. student at the Institute of Microsystems and Microelectronics from the Swiss Federal Institute of Technology Lausanne (Ecole Polytechnique Fédérale de Lausanne). His research interests are on the microfabrication and the characterization of electrophoretic microsystems.

Yves Burri was born in Lausanne, Switzerland, in 1980. He completed his Master degree in Microengineering at the Swiss Federal Institute of Technology Lausanne (Ecole Polytechnique Fédérale de Lausanne) in 2005. The subject of his diploma work, which he carried out at the Institute of Applied Optics, was on the modification of wetting properties of polymers by excimer laser micromachining.

Martin A.M. Gijs received his degree in physics in 1981 from the Katholieke Universiteit Leuven, Belgium and his Ph.D. degree in physics at the same university in 1986. He joined the Philips Research Laboratories in Eindhoven, The Netherlands, in 1987. Subsequently, he has worked there on micro- and nano-fabrication processes of high critical temperature superconducting Josephson and tunnel junctions, the microfabrication of microstructures in magnetic multilayers showing the giant magnetoresistance effect, the design and realization of miniaturized motors for hard disk applications and the design and realization of planar transformers for miniaturized power applications. He joined the Swiss Federal Institute of Technology Lausanne (Ecole Polytechnique Fédérale de Lausanne) in 1997 as a professor in the Institute of Microelectronics and Microsystems, where he is responsible for the Microsystems Technology laboratory. His main interests are in developing technologies for novel magnetic devices, new microfabrication technologies for microsystems fabrication in general and the development and use of microsystems technologies for biomedical applications in particular

For copyright reasons, this document can neither be copied nor printed.

This article is available online at the following address:

[doi: 10.1016/j.snb.2005.01.005](https://doi.org/10.1016/j.snb.2005.01.005)